

A&A manuscript no. (will be inserted by hand later)
Your thesaurus codes are: 10.19.3; 13.09.1

Evidence for a two-armed spiral in the Milky Way

R. Drimmel

Osservatorio Astronomico di Torino, 10025 Pino Torinese, Italy
 email: drimmel@to.astro.it

Received ; accepted

Abstract. Emission profiles of the Galactic plane in K and at $240\ \mu\text{m}$ are presented, and features associated with the tangents of the spiral arms are identified. In the K band, which traces stellar emission and suffers little from absorption, features associated with the arm tangents indicate that a two-armed logarithmic spiral dominates the nonaxisymmetric structure of the Milky Way. In contrast, the $240\ \mu\text{m}$ emission from dust entrained in the interstellar gas is consistent with a four-armed model, in concordance with radio data and optical spiral tracers. This suggests that the non-axisymmetric mass perturbation responsible for the four-armed spiral structure in the gas has a two rather than four-armed structure.

Key words: Galaxy: structure; Infrared: galaxies

1. Introduction

A nearly ubiquitous and prominent feature of disk galaxies is the presence of spiral arms. Unfortunately the spiral arm structure of our own Galaxy is much less obvious due to our obscured view from within its disk. Luminous spiral arm tracers, especially HII regions, have been used to effectively map the main spiral arms of our Galaxy (Georgelin and Georgelin 1976), with the help of kinematic distances. Similar mappings have been made with components of the gaseous medium, such as HI and CO, and more recently the direction of the galactic magnetic field, which is presumably aligned with the arms, has been inferred from studies of pulsar radio observations. From such studies it is usually inferred that the Milky Way has four spiral arms with a pitch angle of approximately 12° (see Vallee 1995 for a recent review). Apart from such spatial mappings, three of the spiral arms directly evidence themselves in Galactic plane emission profiles as features in the directions of the arm tangents where the column flux density of the associated material is greatest.

If the spiral structure is produced by a non-axisymmetric component in the stellar distribution, where the majority of the disk mass resides, then the observed gas and optical spiral tracers make up a small fraction of

the total mass actually associated with the spiral arms. To directly observe the mass associated with spiral structure one must observe the old stellar population, which is best traced by K band imagery (Rix and Zaritsky 1995). Alternatively, the spiral structure could be produced by self-propagating star formation in a differentially rotating medium, which has been shown with simulations to produce spiral arms (Seiden et al. 1979, Jungwiert and Palous 1994). In this case the spiral pattern in K would be produced solely by young stars, which can contribute a significant fraction of the K band light in star forming regions (Rhoads 1998), and will have a form consistent with the optical spiral tracers.

In this letter the K band and $240\ \mu\text{m}$ emission profiles of the Galactic plane are recovered from COBE/DIRBE data, and considered with regards to the spiral structure of the Milky Way. In the following section features associated with spiral arm tangents are identified, and in Sect. 3 the number and position of the tangents are interpreted with a simple logarithmic spiral model.

2. Galactic plane emission profiles

Galactic plane (GP) emission profiles in the K and $240\ \mu\text{m}$ bands were constructed from the 'Zodi-Subtracted Mission Average (ZSMA)' sky maps produced from the COBE/DIRBE data (Kelsall et al. 1998). From the high resolution intensity maps (pixel width $\approx .35^\circ$) pixels within three degrees of the GP where integrated over galactic latitude after reprojecting the data into a Galactic Mollweide projection, using the UIDL analysis package developed by NASA's Goddard Space Flight Center. The resulting emission profiles (integrated intensity) are shown for galactic longitudes $|l| < 90^\circ$ in Figure 1. The K band emission profiles for $|b| > 3^\circ$ show no evidence of spiral arm features, with the exception of longitudes $-60 > l > -90^\circ$.

Emission within 15° of the Galactic center (GC) is dominated by light from the bulge of the Galaxy and absorption from its associated dust lanes, while the very broad and prominent feature at approximately 80° in the $240\ \mu\text{m}$ band is the Orion arm. This arm is a local and rela-

tively minor structure in the Galactic disk and not a major spiral arm (Georgelin & Georgelin 1976); it is prominent only by virtue of our proximity and will not be considered further. I only mention here that its counterpart, centered at $l \approx -100^\circ$, is just outside the right bounds of the figure. Neither do I attempt to identify features associated with this local arm or the Galactic bulge.

Features associated with the tangents to the major spiral arms are expected appear in the galactic longitude range $l > -80^\circ$, $l < 60^\circ$. In this longitude range three types of features are identified and their peaks indicated with vertical lines in Fig. 1: broad ($\Delta l \approx 10^\circ$), prominent features in the K band; strong narrow features in K; and peak emission of broad features at $240 \mu\text{m}$. At negative galactic longitudes the spiral structure of the Galaxy shows itself clearly in K as two broad features at ≈ -20 and -50° , and two narrow features at $\approx -70^\circ$, while the $240 \mu\text{m}$ emission has a distinct sawtooth profile. At positive longitudes the spiral arms are less evident, with a single prominent feature at $\approx 30^\circ$ double peaked in both the K and $240 \mu\text{m}$ bands. In K the appearance of a double peak can be attributed to absorption, as the $240 \mu\text{m}$ peak at 31° exactly corresponds to the “valley” between the peaks seen in K.

The identified features can be grouped by proximity in longitude in the following manner: at negative galactic longitudes there are three groups, labeled “T”, “S₂” and “C₂”, while at positive longitudes there are the groups “S₁” and “C₁”. Though the C₁ group consists of only a single feature at $240 \mu\text{m}$ it is labeled to facilitate the following discussion. I consider the narrow feature at 42° not to be sufficiently close to other features to be part of a group and leave it unlabeled. With the exception of C₁, each group consists of both $240 \mu\text{m}$ and K band features and span approximately 10° or more in longitude. All other unlabeled features in the K band, in the considered longitude range, have a relative peak to local background signal of less than one fourth.

Emission profiles at other wavebands have not been presented here. In the far-infrared COBE also observed at 100 and $140 \mu\text{m}$, which present very similar GP profiles as the $240 \mu\text{m}$ data. In the near-infrared J, L and M band observations were made, but these are not as cleanly interpreted. The M band is contaminated with Zodiacal emission, while the J band suffers significantly from the effects of absorption in the GP. The L band is in principle more transparent than the K band, however, it is not as reliable a tracer of the stellar mass in the GP as it suffers from molecular emission from polycyclic aromatic hydrocarbons (Dwek et al. 1997). For instance, in L the S₁ feature appears as a single peak, suggesting absorption at play in K, while the S₂ feature appears double peaked, the second peak appearing at precisely the longitude of the $240 \mu\text{m}$ peak; this is a clear indication of L band emission associated with the dust.

3. Interpretation

Each group of features in the GP profiles can be identified with a spiral arm tangent. Three of these groups possess broad K band features: S₁ and S₂ are tangents of the Scutum arm, while the third, T, is the Three-kiloparsec arm. The remaining groups, C₁ and C₂, can be identified as tangents to the Sagittarius-Carina (Sag-Car) arm, though there are important differences in their characteristics with respect to the others in the K band. First, the feature at C₂ has a distinctly different character than the broad features mentioned above, being composed of two narrow features. (The profile for $|b| < 9^\circ$ does not blend or enhance these features above the background.) These narrow features could be combined and considered as a single feature, but its apparent width would still be considerably less than the broad tangent features if removed to similar heliocentric distances (from $.4 - .5$ to $.8 - 1.0 R_\odot$). More serious is the absence of a significant feature in K at $\approx 50^\circ$, also noted in other infrared studies (see Table 1 of Ortiz and Lepine 1993). If the Sag-Car arm was of similar amplitude as the Scutum arm it would produce a tangent feature at $\approx 50^\circ$ of similar amplitude as the S₂ feature, since spiral arm tangents at $\pm 50^\circ$ would have approximately the same galactocentric distance.

From the galactic longitudes of two tangents the parameters of a logarithmic spiral described by $r = Ae^{-a\phi}$ can be determined, where (r, ϕ) are galactocentric cylindrical coordinates. Geometrical considerations give the tangent of the pitch angle p , without approximation, as

$$\tan p = a = \frac{\ln\left(\frac{\sin|l_-|}{\sin l_+}\right)}{\pi - (l_+ - l_-)}, \quad (1)$$

where l_- and l_+ are the longitudes of the tangents at negative and positive longitudes respectively. Using the K band S₁ and S₂ features at $(l_+, l_-) = (27, -53)^\circ$, one arrives at $p = 17.9^\circ$. However, if the double peak of the S₁ feature is due to strong absorption, then its true tangent may be at $l_+ = 30^\circ$ longitude. In this case $p = 15.5^\circ$. In addition, a bias is introduced in the apparent tangent direction as the integrated emission comes from a curved structure with finite width. The peak emission is thus displaced toward the GC, the direction of curvature for the arm. A two degree uncertainty has been estimated for the S₂ tangent longitude due to this bias and possible absorption effects.

The galactic longitude of other arm tangents can be found by using the pitch angle as found above and numerically solving for θ in the equation

$$e^{-a\theta} \sin \theta = e^{a(\Delta\phi - \theta_0)} \sin \theta_0, \quad (2)$$

the longitude angle θ_0 being a given tangent. Using the position of the S₂ tangent for θ_0 and $\Delta\phi = -\pi$, the tangent for the counter spiral of the Scutum arm is found to be at $-20.3 < \theta < -22.8^\circ$, corresponding well to the observed

Fig. 1. Galactic plane ($|b| < 3^\circ$) emission profiles for K band (squares; left vertical scale) and at $240\ \mu\text{m}$ (triangles; right vertical scale) on a logarithmic scale. Diamonds at $l < -60^\circ$ show K band emission integrated over $|b| < 9^\circ$. Peaks of major features are identified with vertical lines: broad, prominent features in K (bold solid lines); strong, relatively narrow features in K (dash-dotted lines); broad features at $240\ \mu\text{m}$ (dashed lines). These features are grouped and labeled according to proximity in longitude. The horizontal error bars above the K band profile show the tangent locations of a two-arm logarithmic spiral assuming the uncertainties shown for the S_1 and S_2 tangents in K, while those below the $240\ \mu\text{m}$ profile show the tangent locations of a four-arm spiral, assuming the indicated uncertainties for the S_2 and C_2 tangent locations at $240\ \mu\text{m}$. The emission within 15° of the Galactic center is dominated by the bulge, while the $240\ \mu\text{m}$ feature at 80° is the (local) Orion arm.

longitude of the Three-kiloparsec arm tangent. A second tangent from this arm is not expected at positive galactic longitudes, as it would pass beyond the Solar Circle.

At $240\ \mu\text{m}$ a four-armed model can be applied. The features with the best defined peaks at this wavelength are S_2 and C_2 , tangents of adjacent arms. Setting $\Delta\phi = -\pi/2$ in Eq. 2 one can retrieve a formula similar to Eq. 1 for a , and use the same approach as above to derive the other arm tangents. Assuming a two degree uncertainty in the positions of the S_2 and C_2 peaks, the pitch angle is found to be between 11.5 and 14.2° , consistent with

previous determinations. The locations of the predicted arm tangents are shown in Fig. 1.

4. Discussion

A comparison of the spiral arm features in the K band and $240\ \mu\text{m}$ emission profiles show important differences. The broad, prominent features in K are consistent with a two-armed spiral model, and show significant offsets from associated $240\ \mu\text{m}$ features, while the $240\ \mu\text{m}$ emission is consistent with the traditional four-arm model. Specifically, there are no significant features at approximately

50 and -35° in K as would be expected from a four-arm model, while the C_2 (Sag-Car) feature shows distinct differences in relative size and form from the three broad features at S_1 , S_2 and T.

The disparity between the $240\ \mu\text{m}$ and K band emission is most cleanly interpreted as indicating that the diffuse stellar emission associated with the arms is not primarily from young stars, but from a nonaxisymmetric density variation in the old stellar population dominated by a two-arm structure. This interpretation is consistent with the distribution of bright near-infrared point sources in the GP, which can be modeled with a traditional four-armed spiral component restricted to the distribution of the youngest stellar populations (Wainescoat et al. 1992; Ortiz and Lepine 1993; Hammersley et al. 1999); the brightest (youngest) stars show the same structure as the optical spiral tracers, in contrast to the fainter (older) stars as evidenced by the diffuse near-infrared emission. Fig. 2 compares the two-arm spiral seen in the diffuse K band emission with those mapped by HII regions (Taylor and Cordes 1993).

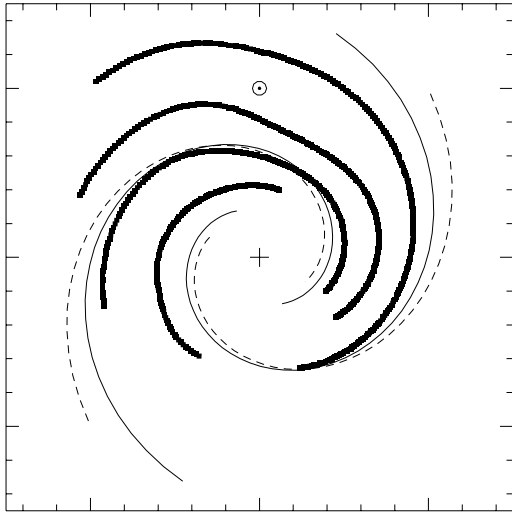


Fig. 2. The two-arm spiral seen in K compared with those seen in the optical (bold lines), as traced by observed HII regions. Solid and dashed lines show the spirals with the minimum (15.5°) and maximum (19°) pitch angles permitted by the positions of the observed K band tangent directions and their uncertainties. The HII arms as illustrated are sparse in the quadrant opposite the Sun (\odot) due to lack of data.

The spiral structure suggested by the K band emission profile for our Galaxy is consistent with near-infrared observations of external galaxies, in that the arms are seen to be broad, well described as logarithmic, and more open than their counterparts at optical wavelengths (Rix and

Zaritsky 1995; Grosbol and Patsis 1998). Also worth noting is that two-armed modes are most common in K band observations of external disk galaxies, regardless of their structure at visible bands, which often can show little correlation with the spirals in the near-infrared (Seigar and James 1998). The contrast between the optical and infrared spiral structure can be understood by remembering that optical spiral tracers are products of star formation in the gaseous arms. The optical spiral tracers, with the dust emission and bright infrared point sources, thus trace the response of the gas to an underlying nonaxisymmetric stellar (mass) distribution; what is unique about the diffuse K band emission is that it principally traces this mass distribution.

The differences in the nonaxisymmetric structure in the gas and stars noted by the above extragalactic studies and in this contribution indicate that the hydrodynamical response to a given potential is not necessarily a simple one. It has been noted in hydrodynamical simulations that the gaseous response to a barred potential can have an extended four-armed spiral structure (Englmaier and Gerhard 1999; Fux 1999), while Patsis et al (1997) have reproduced extensive interarm features with two-armed potentials. These simulations suggest an explanation for the relative weakness of the Sag-Car arm: it is an inter-arm or secondary arm structure, possibly bifurcating from one of the primary arms of the Galaxy. However, to date dynamical models of the Milky Way's stellar disk that include spiral arms have used the tangents seen in optical spiral tracers *as constraints* (Amaral and Lepine 1997). The disparity between the diffuse K band and optical/gas spirals suggest that near-infrared observations will provide crucial information for reconstructing the dynamical and hydrodynamical processes responsible for producing spiral structure.

Acknowledgements. For useful discussions and encouragement the author would like to acknowledge David Spergel, Ortwin Gerhard and Mario Lattanzi.

References

- Amaral L.H., Lepine J.R.D., 1997, MNRAS 286, 885
- Dwek E., Arendt R.G., Fixsen D.J., et al., 1997, ApJ 475, 565
- Englmaier P., Gerhard O., 1999, MNRAS 304, 512
- Fux R., 1999, A&A 345, 787
- Georgelin Y.M., Georgelin Y.P., 1976, A&A 49, 57
- Grosbol P.J., Patsis P.A., 1998, A&A 336, 840
- Hammersley P.L., Cohen M., Garzón F., et al., 1999, MNRAS 308, 333
- Jungwiert B., Palous J., 1994, A&A 287, 55
- Kelsall T., Weiland J.L., Franz B.A., et al., 1998, ApJ 508, 44
- Ortiz R., Lepine J.R.D., 1993, A&A 279, 90
- Patsis P.A., Grosbol P., Hiotelis N., 1997, A&A 323, 762
- Rhoads J.E., 1998, AJ 115, 472
- Rix H.W., Zaritsky D., 1995, ApJ 447, 82
- Seiden P.E., Schulman L.S., Gerola H., 1979, ApJ 232, 702
- Seigar M.S., James P.A., 1998, MNRAS 299, 685

Taylor J.H., Cordes J.M., 1993, ApJ 411, 674

Vallee J.P., 1995, ApJ 454, 119

Wainscoat R.J., Cohen M., Volk K., et al., 1992, ApJS 83, 111